Cerebral Cortex August 2008;18:1843–1855
doi:10.1093/cercor/bhm213
Advance Access publication December 3, 2007

Effects of Working Memory Load on Oscillatory Power in Human Intracranial EEG

Jed A. Meltzer[1], Hitten P. Zaveri[2], Irina I. Goncharova[2], Marcello M. Distasio[3], Xenophon Papademetris[4,3], Susan S. Spencer[2], Dennis D. Spencer[5] and R. Todd Constable[1,3,4,5]

[1]Interdepartmental Neuroscience Program, [2]Departments of Neurology, [3]Biomedical Engineering, [4]Diagnostic Radiology and [5]Neurosurgery, Yale University, New Haven, CT 06510, USA

Studies of working memory load effects on human EEG power have indicated divergent effects in different frequency bands. Although gamma power typically increases with load, the load dependency of the lower frequency theta and alpha bands is uncertain. We obtained intracranial electroencephalography measurements from 1453 electrode sites in 14 epilepsy patients performing a Sternberg task, in order to characterize the anatomical distribution of load-related changes across the frequency spectrum. Gamma power increases occurred throughout the brain, but were most common in the occipital lobe. In the theta and alpha bands, both increases and decreases were observed, but with different anatomical distributions. Increases in theta and alpha power were most prevalent in frontal midline cortex. Decreases were most commonly observed in occipital cortex, colocalized with increases in the gamma range, but were also detected in lateral frontal and parietal regions. Spatial overlap with group functional magnetic resonance imaging results was minimal except in the precentral gyrus. These findings suggest that power in any given frequency band is not a unitary phenomenon; rather, reactivity in the same frequency band varies in different brain regions, and may relate to the engagement or inhibition of a given area in a cognitive task.

Keywords: alpha, BOLD, ECoG, fMRI, gamma, Sternberg, theta

Introduction

Oscillatory activity in field potential recordings has been the subject of numerous studies in humans, both noninvasive (electroencephalography [EEG] and magnetoencephalography [MEG]) and invasive, using as subjects epilepsy patients who are undergoing intracranial EEG recordings for localization of the seizure onset region prior to surgical resection. Although changes in oscillatory power, both positive and negative, are commonly seen in cognitive tasks, interpretation of such effects is not straightforward, as the relationship between neuronal oscillations and cognitive processes is uncertain. It is also unknown to what extent a correspondence exists between oscillatory changes and other measures of neuronal activity, such as spike rate and the metabolic signals seen in functional magnetic resonance imaging (fMRI) and positron emission tomography (PET). Recent studies have suggested that the relationship between oscillatory power and the blood oxygen level–dependent (BOLD) signal in fMRI is frequency dependent, with negative correlations being seen in lower frequency ranges, such as the theta (4–7 Hz) and alpha (8–12 Hz) bands (Goldman et al. 2002; Singh et al. 2002; Laufs et al. 2003; Moosmann et al. 2003; Mizuhara et al. 2004; Brookes et al. 2005; Meltzer et al. 2007), and positive correlations at higher frequencies including the gamma band (~30–70 Hz) (Foucher et al. 2003; Brookes et al. 2005; Mukamel et al. 2005; Niessing et al. 2005).

As cognitive tasks in fMRI typically evoke both positive and negative signal changes in different brain regions (e.g., Shulman et al. 1997; Fox et al. 2005), it may be expected that frequency-specific changes in oscillatory power evoked by a task may also vary regionally throughout the brain. Nonetheless, task-evoked changes in specific frequency bands are commonly reported with a single directionality in most noninvasive studies (e.g., Gevins et al. 1997; Jensen et al. 2002; Foucher et al. 2003). This may be due to the relatively low spatial specificity of surface recordings, in which the most powerful and spatially synchronous intracranial sources may dominate the recording, preventing a fine-grained analysis of reactivity in different regions. In the current study, we performed cognitive tests in epilepsy patients undergoing intracranial EEG monitoring as part of their evaluation for possible surgery. These recordings offer the chance to evaluate the reactivity of brain rhythms across the frequency spectrum, with a greater level of anatomical specificity than that available from surface recordings. In lower frequency ranges, spanning the theta and alpha bands, we have found evidence of strong reactivity of opposite directionality in different regions. At some electrode sites, we observed systematic increases in power with greater working-memory load, whereas decreases were observed at other sites. The occurrences of increases and decreases were not random, but rather demonstrated marked regional specificity.

The Sternberg working-memory task is a popular paradigm in cognitive neuroscience, as it allows the experimenter to parametrically manipulate a single variable, memory load, while keeping all other components of the task constant. In this task, a subject keeps a list of items (such as digits, letters, or spatial locations) in working memory during a delay period, after which he or she must indicate whether or not a specific probe item is on the list. The number of items can be manipulated, allowing the assessment of physiological activity parametrically modulated by memory load. Parametric increases in theta power with memory load have been detected in MEG (Jensen and Tesche 2002) and EEG (Onton et al. 2005), whereas another EEG study reported an increase in the alpha range (Jensen et al. 2002). Although fMRI studies have mostly reported increases in the BOLD signal with greater memory load, it is unknown whether memory load–dependent increases in oscillatory power are generated in the same regions as load-dependent BOLD signal changes. However, preliminary evidence suggests that BOLD and low-frequency EEG power (theta and alpha ranges) may be anatomically dissociated. fMRI studies of the Sternberg task have detected load-dependent effects in the delay period primarily in lateral frontal and parietal regions (Rypma et al. 1999; Jha and McCarthy 2000; Kirschen et al. 2005; Narayanan et al. 2005; Zarahn et al. 2005).

In contrast, the MEG and EEG studies mentioned above have suggested that the sources of increased oscillatory power lie in midline structures. Numerous EEG/MEG studies have indicated that frontal theta power increases detectable in cognitive tasks are generated in the medial prefrontal cortex and/or anterior cingulate (Asada et al. 1999; Ishii et al. 1999; Luu et al. 2004; Onton et al. 2005), and these findings have been corroborated by direct intracranial recordings in human (Uchida et al. 2003; Wang et al. 2005) and monkey (Tsujimoto et al. 2006). Alpha power seems to be generated in multiple cortical locations, but source localization studies have consistently identified midline parietal–occipital sources among the strongest generators (Ciulla et al. 1999; Yamagishi et al. 2003), whereas the parietal–occipital source has also been identified as the origin of alpha activity that is sensitive to cognitive manipulations (Vanni et al. 1997), including memory load–dependent power increases in the Sternberg task (Tuladhar et al. 2007).

Although increases in low-frequency power with memory load have been observed in several noninvasive studies, a series of reports from a group conducting invasive recordings of the Sternberg task have not been entirely consistent with these findings. Power increases with memory load were detected instead in the gamma band in a study of 2 subjects (Howard et al. 2003). In the theta band, a phase reset with stimulus presentation (Rizzuto et al. 2003) and a gating of power during the delay period (Raghavachari et al. 2001) have been reported, but no effect of memory load on the amplitude of theta oscillations in the delay period has been reported in these studies. Invasive studies are not totally comparable with noninvasive studies, having greater sensitivity to activity generated locally (e.g., Raghavachari et al. 2006), whereas scalp recordings tend to be dominated by activity coherent over a larger scale. However, the inconsistency across studies may also be attributable to differences in the experimental design, which are considerable. Given the fairly low number of subjects in the previous intracranial EEG studies, it is possible that load-dependent modulation at lower frequencies exists, but was not readily detectable in the paradigm used. For instance, Howard et al. (2003) report seeing both increases and decreases in theta power, but the number of electrodes involved was too few to draw firm conclusions about the relationship of theta power to memory load, whereas power in the gamma band exhibited a consistently positive correlation with memory load. Axmacher et al. (2007), recording mainly from the medial temporal lobe, also observed gamma increases with memory load, but no significant main effects were observed in lower frequency bands. Another recent study has also identified intracranial gamma power increases during the encoding period of the Sternberg task, specifically for stimuli that are cued to be remembered versus those that are to be ignored (Mainy et al. 2007).

In a previous study (Meltzer et al. 2007), we conducted both fMRI and EEG measurements of the Sternberg task in 18 normal volunteers, using intersubject differences in EEG reactivity as a means to evaluate the relationship between theta and alpha power and the BOLD signal. In that study, most subjects exhibited robust positive BOLD activation in lateral frontal and parietal regions, in response to greater memory load. Additionally, a minority of subjects exhibited increases in frontal midline theta power in EEG, and these subjects tended to also exhibit fMRI deactivation in frontal midline cortex, resulting in an observed negative correlation between frontal theta power and BOLD. Additionally, negative correlations were observed between posterior alpha power and BOLD in posterior midline cortex.

In the present study, we have obtained data from 14 patients performing the Sternberg task, at a total of 1453 intracranial electrode sites, providing an opportunity to evaluate the intracranial distribution of memory load effects in different frequency bands. The results of our study are largely consistent with those of Howard et al. (2003), in that gamma power tended to increase with memory load, but increases and decreases in the theta and alpha bands were equally prevalent. The relatively large sample size and broad spatial sampling in this study allows us to analyze the anatomical distribution of these effects, to see if power changes of opposite directionality can be anatomically dissociated. Additionally, due to minor differences in neurosurgical technique between our epilepsy center and that of other teams that have conducted previous studies of the Sternberg task, we have been able to obtain extensive coverage of the cortical midline regions, which allows us to test the specific hypothesis that increases in theta and alpha power are preferentially generated in midline structures.

Methods

Subjects

Seventeen subjects were selected from patients undergoing invasive monitoring of seizure activity at Yale New-Haven Hospital, who met the following criteria: minimum age of 14, minimum Wechsler IQ of 80, and verbal memory impairment not greater than 2 standard deviations below the mean on the Buschke selective reminding test. All subjects gave informed consent according to a protocol approved by the Yale University Human Investigation Committee. Two subjects were excluded from analysis because the intracranial EEG data were dominated by large-scale epileptiform activity, as judged by an experienced neurologist. In the other subjects, only individual electrodes were rejected due to suspected contamination from epileptiform activity (see data analysis section below). One further subject was excluded because of low-quality anatomical scans, making it impossible to accurately map the electrodes in standard space. Therefore, the final analysis included 14 subjects (8 females).

Task

A Sternberg working-memory task was employed, similar to that used in a related EEG–fMRI study (Meltzer et al. 2007), but slightly modified to make it easier for patients undergoing intracranial EEG monitoring to perform, given that some patients may have slight cognitive impairments as a result of epilepsy, and are performing the task under less-than-ideal conditions. Generally, subjects were regularly taking narcotic pain medication while recovering from surgical implantation of intracranial electrodes, and were also undergoing a tapered withdrawal from their customary regime of antiepileptic drugs in order to induce seizures. Memory load levels of 1, 2, and 4 digits were used. On each trial, a "start" cue was presented to mark the start of a new trial and reinforce the fact that the previous numbers could be disregarded. Next, the array of 1, 2, or 4 digits was presented for 4 s. Digits were then replaced by a matching array of 1, 2, or 4 horizontal lines indicating the delay period, which lasted 6 s. Next, the probe digit appeared between 2 question marks, and subjects responded with a button press to indicate whether or not the digit was in the array. Subjects had a maximum of 3 s to respond before the next trial began. The task was administered as a series of twelve 4-min sessions, each including 15 trials. The memory load was kept constant during each 4-min session, and 4 sessions of each load level were conducted. The task was administered on a laptop computer placed directly on the patients lap or on a telescoping table in front of them, according to their preference. To maximize patient comfort, we did not apply the

usual strict control of responses typical of laboratory experiments with healthy subjects. Subjects were allowed to use either hand, or both, according to their preference. As activity during the delay period was the topic of interest, possible confounds from motor responses were not relevant. Furthermore, patients were not instructed to respond as fast as possible, but to try to maximize accuracy while responding within the 3-s time limit.

Recordings

Intracranial EEG was recorded with a 128-channel Ceegraph clinical monitoring system (BioLogic Systems Corp., Mundelein, IL). Patients were implanted with square grids and rectangular strips of stainless steel subdural electrodes on frontal, temporal, parietal, occipital, and midline (interhemispheric) surfaces, and, in some cases, with multi-contact depth electrodes in the medial temporal lobe. Each subdural electrode had an exposed surface of 2.3 mm in diameter, spaced at 1-cm intervals. The placement of electrodes within each patient was determined solely by clinical criteria; however, the routine clinical use of broad anatomical coverage for intracranial recordings at Yale provided a large sample of electrophysiological data from tissue outside of the epileptogenic zone. Recordings were monopolar, referenced to a single titanium peg electrode placed between the inner and outer laminae of the skull, distant from the study electrodes within the limits of the craniotomy. Signals were digitized at 256 Hz. When available, an electronic marker signal was delivered from the stimulus presentation computer into the data stream of one EEG channel as a timestamp at the onset of each trial. In some subjects (8 out of 14), this mechanism was not available, in which case the beginning of each recording session was marked by the experimenter pressing the seizure event button. Because the latter procedure has a temporal precision of 1 s, our chosen data analysis routines reflected this uncertainty.

Power Spectral Analysis

Digitized intracranial EEG was imported into MATLAB (Mathworks, Natick, MA) for analysis, using EEGLAB software (Delorme and Makeig 2004) and custom-written scripts. Electrode signals were visually screened for severe artifacts, and contaminated trials were excluded. Additionally, individual electrodes were excluded from analysis on the basis of 3 other criteria: showing evidence of interictal epileptic activity, overlying the seizure onset zones as defined by the clinical team, and overlying areas of gross structural abnormality as seen on the anatomical scans.

The primary measure of interest for this study was oscillatory power as a function of memory load during the delay period of the Sternberg task. The middle 5 s of the 6-s delay period from each trial were submitted to multitaper spectral analysis, to estimate the power spectrum. Spectra were averaged within each load condition (1, 2, and 4 digits). Like most stochastic natural processes, intracranial EEG is characterized by a "$1/f$" or "red noise" spectrum, meaning that power is greatest at lower frequencies and smoothly declines with increasing frequency. As oscillatory processes are manifested as peaks in the spectrum that emerge from the $1/f$ background, they are optimally detected by preprocessing the raw spectra to remove the background red noise. Therefore, the estimated spectra were "whitened" by fitting each electrode's average power spectrum (across all conditions) to a $1/f$ distribution described by the equation:

$$P(f) = Af^{\alpha}$$

where f is frequency, $P(f)$ is the power at each frequency (in units of squared millivolts), and A and α are constants fit by a nonlinear optimization program (fminsearch in MATLAB). This fitted spectrum was subtracted from each trial, thus producing a "whitened" power spectrum. Because this subtraction of a constant was applied to each trial equally, it does not affect the nonparametric statistical analysis that was subsequently employed to test for changes in power associated with different levels of memory load. However, the prewhitening step allows for the detection of spectral peaks corresponding to periodic oscillations (Fig. 1) and transforms the power spectra into a form more convenient for plotting across all frequencies (compare Fig. 1*A,B* with Fig. 1*C,D*).

Detection of Oscillatory Peaks

Although power changes associated with memory load may not necessarily occur at frequencies associated with a local peak in the power spectrum, we were also interested in characterizing what peaks tended to be present in the intracranial EEG data, for qualitative comparison with recordings obtained from noninvasive methods. Typically, human EEG is characterized by a $1/f$ power spectrum, plus a peak at 10 Hz corresponding to the alpha rhythm, and occasionally a second peak in the beta frequency range. However, this may not be the case in intracranial data. To evaluate the frequency distribution of spectral peaks in these data, we applied a peak-detection algorithm to the prewhitened power spectra of each electrode, averaged across trials and conditions. The peak-detection algorithm, part of a freely available Matlab toolbox (http://www.wam.umd.edu/~toh/spectrum/PeakFindingandMeasurement.htm), functions by searching for downward zero-crossings in the smoothed first-derivative of the power spectrum that exceed given slope and amplitude thresholds, which were manually set on the basis of a subset of the intracranial EEG power spectra. Finally, the total number of detected peaks at each frequency across all electrodes was summed across all electrodes in all subjects, producing a histogram of the frequency of occurrence of spectral peaks across the frequency axis from 4 to 50 Hz.

Electrode-wise Statistical Analysis

Because the placement of electrodes varied in each patient, it was not possible to conduct direct second-level statistical analysis across subjects as is conventionally done in noninvasive EEG studies. Instead, statistical analyses were conducted at each electrode independently. Categorical statistical techniques were then applied to characterize the anatomical distribution of significant effects across subjects (see below). As the primary measure of interest in this experiment was increases and decreases in power with greater memory load, we selected a planned comparison of the 1-digit and 4-digit conditions for statistical analysis of load effects. The intermediate 2-digit condition was used primarily for visual confirmation of the parametric nature of the changes. Estimated power spectra had a frequency resolution of 0.5 Hz, and frequencies from 0.5 to 50 Hz were analyzed, for a total of 100 frequency points per electrode. At each electrode and frequency, we computed the Wilcoxon rank-sum statistic on the estimated power values across trials. Wilcoxon statistics were converted into equivalent Z-scores, and the resulting z-values constituted a nonparametric estimate of the statistical evidence for a difference between the 2 distributions, free of distributional assumptions.

This analysis was applied to each electrode and frequency point in parallel, thus it is necessary to control for the inflated false positive rate associated with multiple comparisons. We adopted a bootstrap procedure used in a previous intracranial EEG study (Sederberg et al. 2003), in which 1000 resamplings (with replacement) of the data were generated by randomly assigning trials to the 1-digit and 4-digit category. The same reshuffling was used for all electrodes simultaneously, to control for the fact that different electrodes are not independent of each other. Next, the z-transformed Wilcoxon rank-sum statistic was recomputed for each electrode, frequency, and resampling iteration, so that the empirical null distribution of the statistic could be computed. This computation allowed for the selection of a significance threshold that would set the expected false positive rate at a given level. We chose a rate of 0.001. The presence of an occasional false positive is not a major concern, as our goal was to generate an overall picture of the anatomical distribution of statistically significant power changes, and any individual false positive is unlikely to give a false impression. This is a different situation than other applications of massively univariate multiple testing, such as genetic microarrays, in which each gene is an independent entity whose individual significance has specific implications. Using a higher or lower threshold includes fewer or more electrodes in the significance histograms (Fig. 3) but has virtually no effect on the overall pattern of results.

The significance testing described above was used to detect electrodes at which the power spectrum differed during maintenance of different levels of memory load. Power spectra were computed from data recorded during the delay period of the task, when subjects had

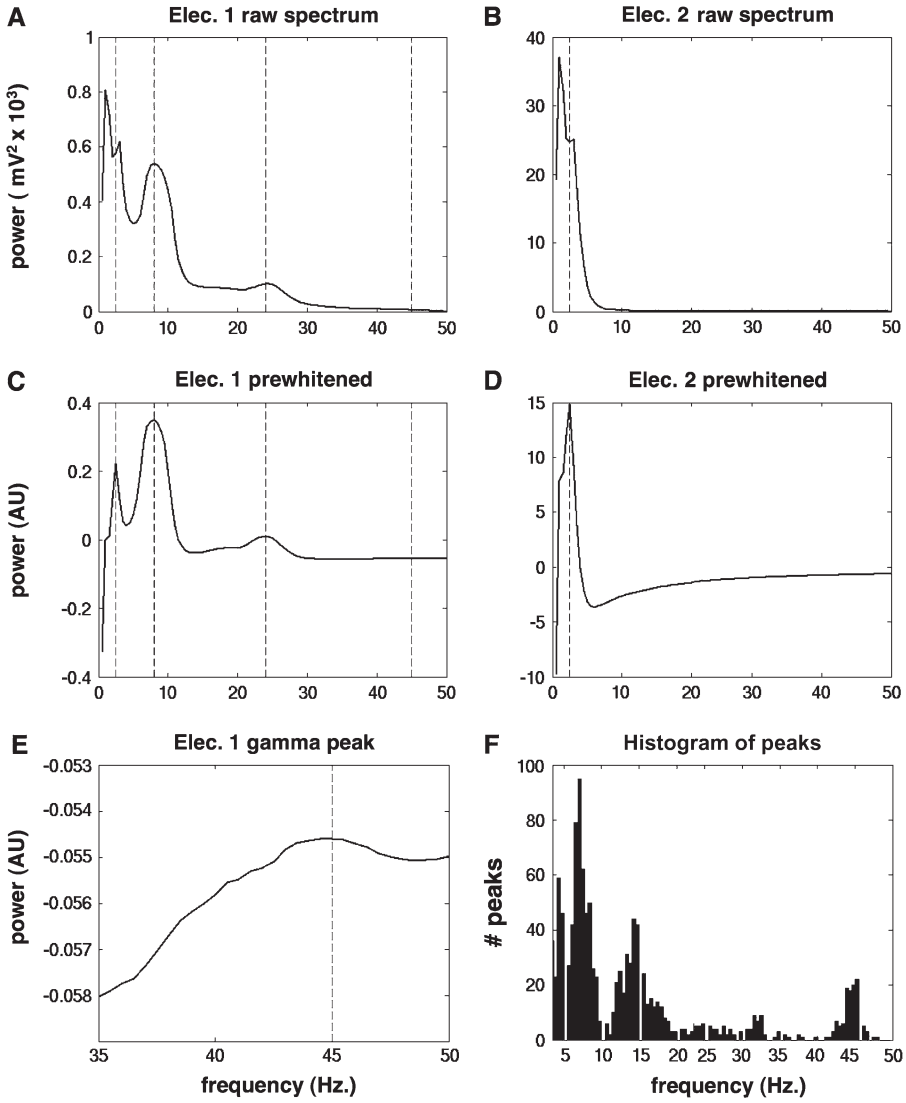

Figure 1. (*A*) Raw power spectrum of a single representative electrode exhibiting multiple oscillatory peaks. Vertical lines indicate peaks detected by an automatic algorithm. (*B*) Raw power spectrum of a second electrode from the same subject, exhibiting no oscillatory peaks except at very low frequencies. (*C*) The power spectrum from the first electrode after application of the "whitening" algorithm (see text). (*D*) The whitened power spectrum of the second electrode. (*E*) Close-up view of the gamma peak from the first prewhitened spectrum. (*F*) Histogram of oscillatory peaks across the frequency spectrum, detected in all 1453 electrodes in the study.

viewed the digit array and were awaiting the probe digit. Because different levels of memory load were administered in blocks (as this arrangement was less confusing for patients), it is possible that the observed changes are not specific to the delay period, but merely reflect sustained effects of attention and effort associated with performance during more difficult task blocks. To rule out that possibility, 2 additional analyses were performed. First, a set of 2-s data segments were extracted from the intertrial intervals, comprising ±1 s around the "start" cue that preceded each digit array. Statistical analyses were then performed on these intertrial data segments identical to those performed on the delay period. If the observed power changes are attributable to sustained effects of attention and effort, then a similar pattern of changes should be detected during the intertrial periods across conditions. If the changes are instead specific to periods of memory maintenance, then we would expect very few significant changes to occur during the intertrial periods.

A second method of evaluating the temporal dependence of power changes is to conduct time–frequency analysis on the 16-s time courses of whole trials. Because the hardware setup for some patients (8 out of 14) did not permit the placement of electronic time markers in the EEG data, temporal accuracy was limited in those cases to ± 0.5 s, thus limiting our ability to meaningfully average time courses across trials. Therefore, time–frequency analysis was not adapted as a primary technique for statistical analysis across electrodes, but was conducted on a subset of electrodes for display purposes (Fig. 2*E*,*F*), allowing us to visualize the divergence of power time courses during the delay period. We used the "Event-related Spectral Perturbation" method ("ERSP," Makeig 1993), implemented in EEGLAB. Epochs were divided into 300 overlapping Hanning-windowed time segments, and the fast fourier transform power spectrum was computed for each segment, yielding a spectrogram, which was then log-transformed. The log-transformed average power spectrum from the prestimulus baseline period was subtracted from each segment's value, yielding the ERSP, an estimate of changes in power normalized to the prestimulus baseline. ERSP values were averaged separately in each condition, and plotted at frequencies corresponding to peaks in the whitened power spectra.

Anatomical Analysis

Electrode localization was performed using the bioimagesuite package developed at Yale University (www.bioimagesuite.org). To determine the location of electrodes included in the analysis, individual electrode

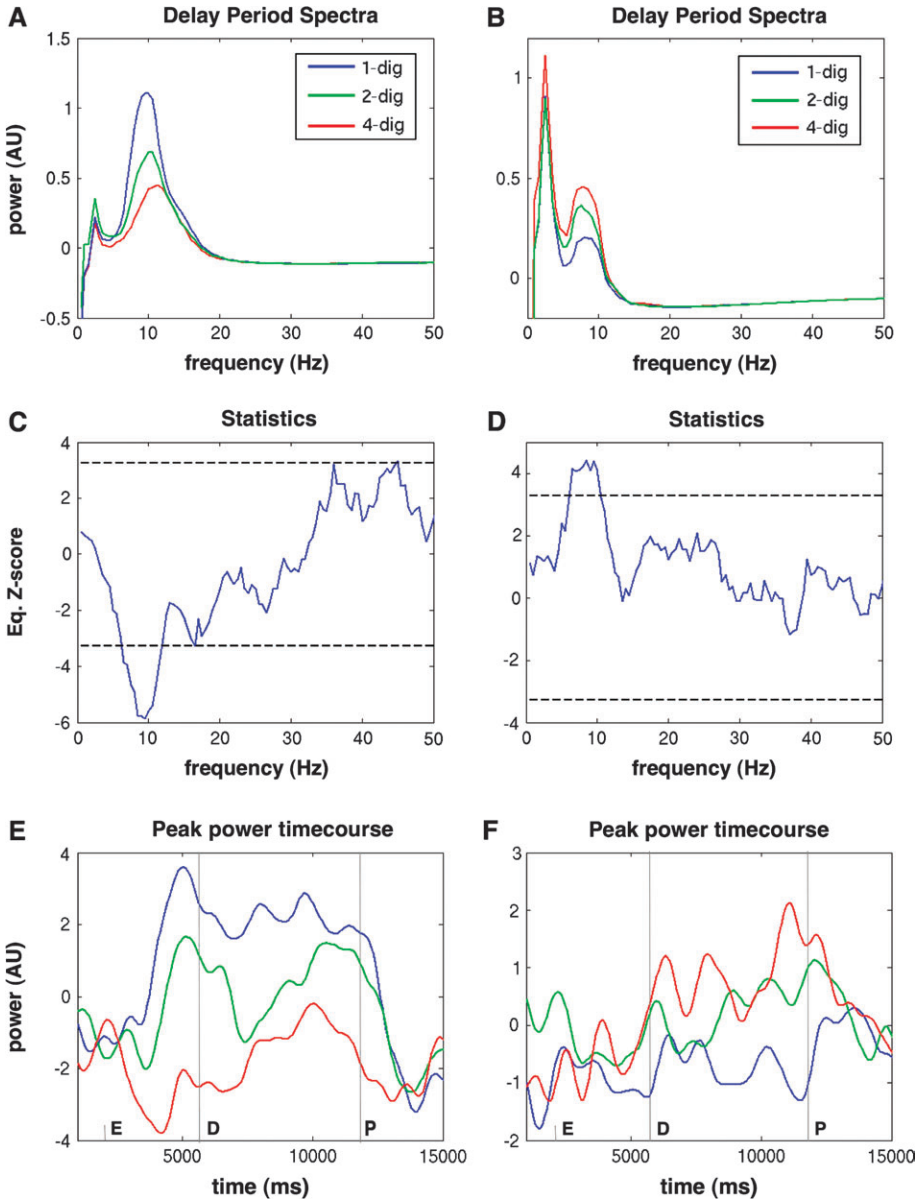

Figure 2. Examples of electrodes showing opposite effects of memory load in the theta/alpha range. (*A*) Whitened power spectra (see Methods) of an electrode in right occipital cortex, with alpha power decreasing with memory load. (*B*) Power spectra of an electrode in left temporal cortex, with a peak overlapping theta and alpha bands increasing with memory load. (*C*) Equivalent *z*-value at each frequency for the same electrode shown in (*A*) (see Methods), showing significant alpha decrease as well as gamma increase. (*D*) Equivalent *z*-values for the electrode in (*B*). (*E*) Time course of power at the alpha peak frequency for the first electrode, demonstrating that power diverges during the delay period (indicated by vertical lines). The letters E, D, and P mark the onset of the encoding period (presentation of the digit array), delay period (offset of the digits), and probe period (onset of the single probe digit). (*F*) Time course of peak power for the second electrode.

locations were marked on postoperative computed tomography (CT) scans. CT scans were registered to postoperative MRI scans using a 6-parameter rigid transformation, and postoperative MRI scans were then registered with preoperative scans using a nonlinear grid-based transformation (Papademetris et al. 2004) to account for the distortion of the brain that occurs as a result of the craniotomy. Finally, the preoperative MRI scans were registered to a reference brain (the "Colin brain," http://www.mrc-cbu.cam.ac.uk), using the same nonlinear technique.

Because the anatomical distribution of electrodes was different in every patient, high-resolution voxelwise statistical analysis was not possible. Nonetheless, the large number of electrode recordings obtained across 14 subjects allowed for a second-level categorical analysis on a broad lobar level, to test for the presence of significant differences in the anatomical distributions of power changes in different frequency bands. Three categories of power spectral changes (theta/alpha increase, theta/alpha decrease, and gamma increase) were defined on the basis of the observed patterns of power changes (see Results and Fig. 3*A*). A primary hypothesis of interest in this study was that increases in low-frequency power would tend to localize to frontal and parietal midline locations, as suggested by previous noninvasive studies of the Sternberg task (see Introduction). Therefore, we defined one region of interest (ROI) to include all electrodes located in the midline region in the frontal and parietal lobes, defined as ±1.5 cm from the midline slice. One categorical analysis simply compared this region to all other parts of the brain. Additionally, we conducted a second exploratory analysis comparing 6 different regions to detect any other salient patterns of anatomical distribution. These regions, illustrated in Figure 4*A*, were as follows: ML: frontal and posterior midline, as described above, OC: occipital, including all electrodes posterior to the

origin of the Sylvian fissure, LF: left frontal-parietal, including all electrodes superior to the Sylvian fissure, lateral to ML on the left, and anterior to the OC, RF: right frontal-parietal, defined like LF, but on the right, LT: left temporal, including all electrodes inferior to the Sylvian fissure and lateral to ML on the left, RT: right temporal, defined like LT, but on the right.

Electrodes in each response category were plotted on an atlas brain (Figs 4*A* and 5) to allow for the visual evaluation of any clustering patterns. For lobar-level statistical analysis, it was necessary to adopt procedures that control for the effects of different subjects on the resultant anatomical patterns. Subjects may vary in the extent to which they increase or decrease power in specific frequency bands, but they also vary greatly in the placement of their electrodes—some have electrodes only on the left or right, and some have many midline electrodes, whereas others have very few. Therefore, there is a possibility that the apparent differences in ROIs are entirely attributable to a subject effect. To control for this possibility, we used the Mantel–Haenszel test (Agresti 2002), which is a multidimensional generalization (for $2 \times 2 \times K$ tables) of the more familiar chi-square test. This procedure tests for an association between 2 binary categorical variables (in this case, presence of an electrophysiological change and ROI) while controlling for a third variable (subject), which may have arbitrarily many levels. Essentially, the association is tested within each subject separately, and the results are combined. This test was used for the comparisons between the midline ROI and all other ROIs. This test also estimates a common odds ratio, indicating the increased likelihood of electrodes within the hypothesized ROI to exhibit a given effect, compared with electrodes in other ROIs.

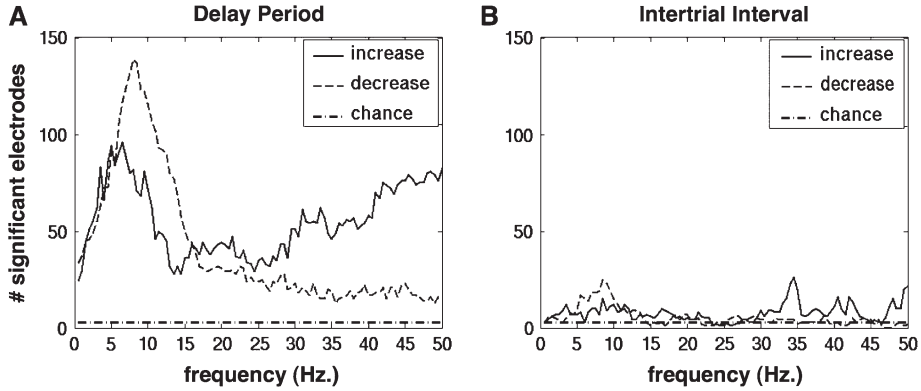

Figure 3. (*A*) Histogram of the total number of electrodes in all subjects showing a significant effect of memory load on oscillatory power at each frequency during the delay period of the Sternberg task. The horizontal line represents the number to be expected by chance alone at the chosen significance level ($P < 0.001$), based on a permutation distribution computed from 1000 random resamplings of the trials in each subject. (*B*) Identical analysis performed on data extracted from the intertrial interval. This serves as a control to confirm that the observed changes are mainly specific to the delay period of the task, rather than being driven by sustained changes in attention or effort over the length of task blocks.

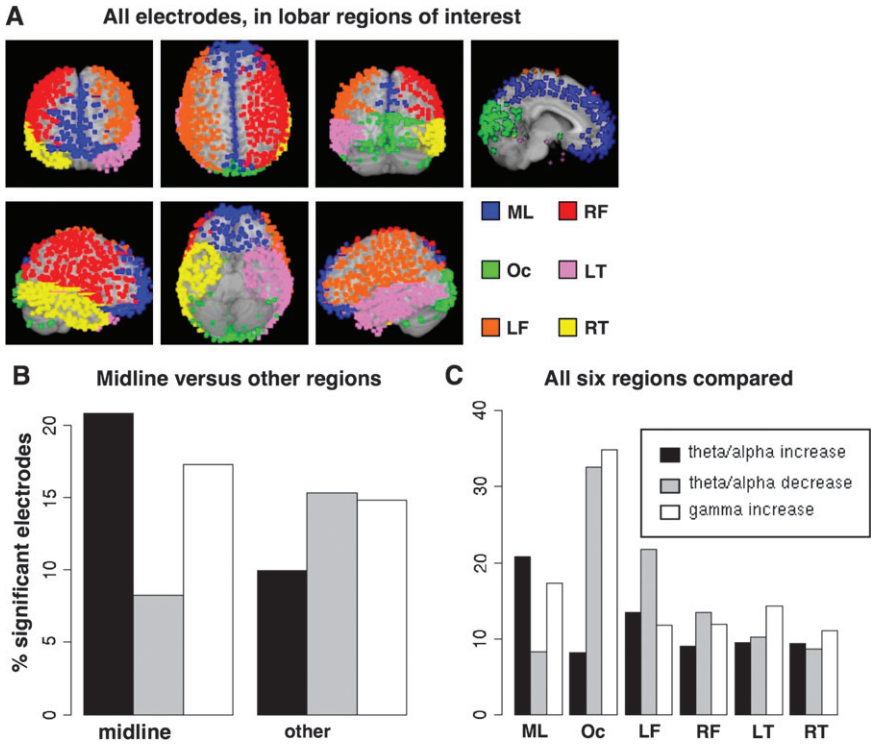

Figure 4. (*A*) All electrodes across 14 subjects that were included in the statistical analyses, with the 6 anatomical ROIs indicated by a color code (see text). (*B*) Proportion of electrodes in the midline frontal/parietal region expressing each category of spectral power change, compared with all other regions. (*C*) Comparison of power changes in all 6 regions. These proportions are combined across different subjects with different electrode placements; see text for details of statistical inference.

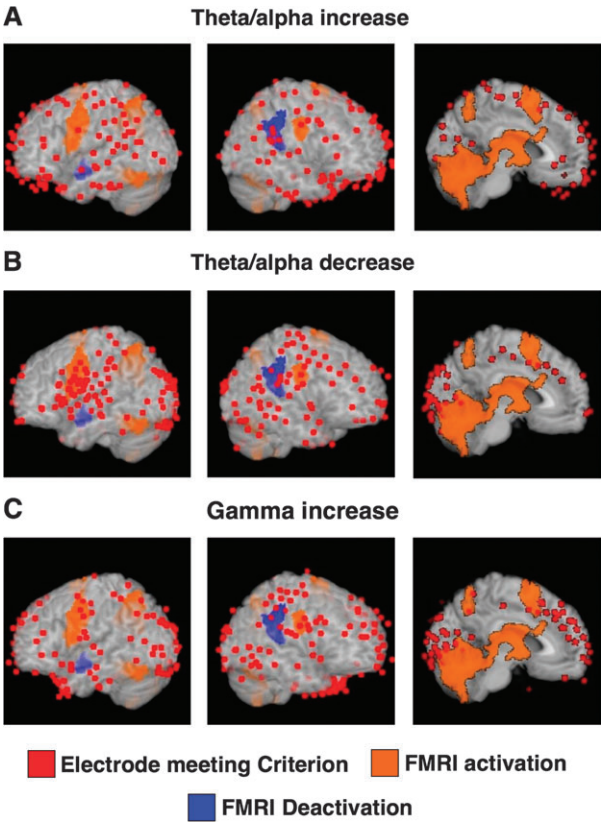

Figure 5. Maps of electrodes exhibiting each category of spectral power change, overlain on an anatomical atlas brain and an fMRI map of delay-period memory load–induced BOLD signal changes obtained from a previous study. (*A*) Electrodes exhibiting an increase in power with memory load in the theta/alpha range (5–13 Hz). (*B*) Electrodes exhibiting a decrease in power with memory load in the theta/alpha range. (*C*) Electrodes exhibiting an increase in power with memory load in the gamma range (30–50 Hz).

For the exploratory comparison across all 6 ROIs, we employed the Cochran-Mantel-Haenzel test (Agresti 2002), which is a further generalization of the chi-square procedure for $2 \times N \times K$ tables, but it does not estimate an odds ratio, because more than 2 regions are being compared.

In addition to the formal categorical statistical tests described above, we also elected to overlay the electrode maps on a thresholded fMRI map derived from our previous EEG–fMRI study of the Sternberg task (Meltzer et al. 2007). That study focused on individual differences, demonstrating negative correlations between BOLD and theta and alpha power induced by greater memory load, primarily in midline structures. Additionally, however, that study generated a map of (mostly positive) BOLD changes associated with greater delay-period memory load, consistently across the cohort of subjects. We have used that map here as an underlay to the electrode maps, so that any obvious overlap between BOLD changes and intracranial EEG power spectrum changes may be appreciated. For details of fMRI acquisition and analysis, the reader is referred to the previous study. Briefly stated, the underlay map is a subtraction of delay-period BOLD signal for 6-digits minus 2-digits, thresholded at $P < 0.01$ voxelwise and cluster-filtered for a whole-brain family-wise error rate of $P < 0.05$.

Results

Behavioral

As we did not strictly control the way that patients physically interacted with the computer to perform the cognitive task (see Methods), the behavioral results of this study serve mainly to confirm that patients performed the task adequately, but cannot be taken as an optimal estimate of reaction time as in traditional experimental psychology. The primary activity of interest in this study is during the delay period of the task, whereas behavioral data are obtained only at the response phase. Intersubject reaction time variance was affected by the fact that some subjects kept their hand on the laptop throughout the experiment, whereas others did not. Consistent with previous reports of the Sternberg task, response time increased linearly with memory load. Mean response times were 1-digit: 1686 ms, 2-digit: 1781 ms, 4-digit: 2020 ms. Repeated measures analysis of variance with subject as a random effect indicated a significant linear increase with memory load of 112 ms per digit ($F_{1,13} = 20.99$, $P < 0.001$). There was no significant effect of load on accuracy, which averaged 92% correct (1-digit: 93%, 2-digit: 92%, 4-digit: 92%, $F_{1,13} = 1.34$, $P = 0.26$). The vast majority of noncorrect trials resulted not from incorrect responses but from failure to respond within the time limit. The linear effect of load on reaction time and lack of effect on accuracy is consistent with our concurrent EEG–fMRI study on healthy controls (Meltzer et al. 2007), although reaction times tended to be higher and accuracy lower in the current study with epilepsy patients compared with control subjects. However, this is to be expected, considering the nonideal conditions under which patients are performing the task, discussed in the methods section. All patients understood the task and performed it with high confidence.

Oscillatory Peak Detection

As an illustration of the peak-detection process, 2 example power spectra from different electrodes in the same subject are illustrated in Figure 1. Figure 1*A* depicts the raw power spectrum (averaged across trials and conditions) from an electrode exhibiting 4 oscillatory peaks, one in a very low frequency, and the others in the alpha, beta, and gamma ranges. Figure 1*B* depicts an electrode with no peaks except for the very low frequency peak. Peaks in the whitened spectra below 4 Hz were detected at most electrodes and are not considered further, as they mostly represent background noise that is not fit by the $1/f$ noise model. Figure 1*C,D* depicts the whitened spectra, which were used as input to the peak-detection algorithm. The whitening makes the peaks into local maxima in the power spectrum, which is not necessarily the case in the presence of the $1/f$ "red noise" background. Figure 1*E* displays a close-up of the gamma band peak for the first electrode.

Figure 1*F* displays a histogram of peaks detected at each frequency across all electrodes included in the analysis. The greatest number of peaks occurs at 7 Hz, with most peaks occurring between 5 and 9 Hz. A second concentration of peaks is seen centered at 14 Hz, which is of course the first harmonic frequency of 7 Hz. A considerable number of peaks were also detected in the gamma band, centered at approximately 45 Hz, as in the example electrode 1. Notably, there are virtually no peaks at 10 Hz, which is typically the most common frequency of peak alpha oscillation in scalp EEG recorded from healthy volunteers. This is a somewhat surprising finding. In fact, we found that most large oscillatory peaks in this dataset covered a fairly wide range that overlapped the theta and alpha bands as they are traditionally defined, but that the peak

frequencies tended to be lower than those typically observed in scalp EEG experiments. There are numerous possible reasons for this, including differences between scalp and intracranial recordings (such as the filtering properties of the skull), subject differences (all of the intracranial subjects suffer from epilepsy), and drug effects (all of the subjects are on antiepileptic medications). Although it is not possible to control for all of these factors in an intracranial EEG study, it is important to note this difference in the baseline spectral characteristics of intracranial recordings compared with scalp EEG recorded from healthy volunteers. Noninvasive studies frequently distinguish between the alpha band (8–12 Hz), which forms a broad spectral peak, and the theta band (~4–7 Hz), which generally does not form a spectral peak. Given that the observed spectral peaks in the intracranial data tended to overlap both of these bands, we did not attempt to distinguish between them in the analysis of load-induced power changes.

Effects of Memory Load

Significant changes in oscillatory power with greater working-memory load were detected in all subjects, in multiple frequency bands. Representative examples from 2 electrodes are displayed in Figure 2.

In both cases, the significant change in power occurs at a peak in the power spectrum overlapping the theta and alpha ranges, between 5 and 11 Hz. Figure 2*A* shows delay-period power spectra from an electrode located in the right occipital lobe that exhibited a decrease in low-frequency power with increasing memory load. Figure 2B shows an electrode from a different subject, located in the left temporal lobe, that displayed the opposite effect, an increase in power with memory load. Figure 2*C*,*D* shows the equivalent *Z*-values arising from the nonparametric statistical procedure used to assess the significance of power changes (see Methods). The dashed line represents the empirically determined significance threshold of $P < 0.001$. Figure 2*D*,*E* displays the temporal evolution of power at the theta/alpha peak, estimated with the ERSP method. These time courses suggest that power is specifically modulated in the delay period of the individual trials, rather than being attributable to sustained changes over the entire block, as confirmed by the contrast between delay-period and intertrial interval changes presented in Figure 3.

A histogram showing the number of electrodes exhibiting a significant increase or decrease in power at each frequency is displayed in Figure 3*A*. In the gamma band, changes were predominantly positive. In lower frequency ranges, however, a more complex pattern emerges. Decreases in power with greater memory load were seen primarily at lower frequencies, with the greatest number of electrodes being significant at 8 Hz. Increases in power are also seen in the same frequency range, at a smaller number of electrodes. The maximum number of electrodes showing a significant increase in low-frequency power occurred at 6.5 Hz, but the distribution of increases and decreases overlaps considerably in this range.

A histogram showing significant changes during the intertrial interval is shown in Figure 3*B*. Changes occurring during the intertrial interval could be attributable to nonspecific processes of arousal and attention taking place over blocks of performance of the more difficult condition. At most frequencies, the number of significant electrodes does not rise above the expected chance level. Some significant changes are detected in the theta and gamma ranges, but the number of electrodes involved is a small fraction of those exhibiting changes during the delay period. Therefore, the vast majority of power spectral changes with memory load observed in this experiment appear to be specifically modulated by the temporal structure of the task.

The frequency distribution of significant power changes with memory load observed here fail to support a distinction between the theta and alpha bands as traditionally defined in scalp EEG studies, confirming the impression of the oscillatory peak-detection analysis, namely that task-modulated oscillations tend to occur in a broad range encompassing both of those bands. Therefore, we make no distinction between these bands in further analyses. The frequency distribution observed here suggests that most memory load-induced power changes fall into 3 categories. We defined the following 3 categories for subsequent analysis of anatomical distributions:

1. Theta/alpha increase: 5-13 Hz.
2. Theta/alpha decrease: 5-13 Hz.
3. Gamma increase: 30-50 Hz

Each electrode was classified into one or more of these categories if the *Z*-value equivalent statistic exceeded the significance threshold for at least 2 consecutive frequencies within the specified bands.

Anatomical Distribution

Figure 4*A* shows the locations of all 1453 electrodes included in the statistical analysis over 14 subjects, showing that most of the cortex was fairly evenly sampled, even though the locations of electrodes in any individual subject were much more limited. We relied on 2 methods to assess the anatomical distribution of power spectral changes in different frequency bands; the first method being formal categorical analysis to allow for statistical inference, and the second being visual inspection of electrode locations in comparison with previously obtained fMRI results, which is informal but potentially more informative. Electrodes in Figure 4*A* are color coded, indicating the spatial extent of the 6 broad anatomical categories that were defined a priori.

Figure 4*B* shows the proportion of electrodes in the ML region and the rest of the brain classified into each category. This refers to the number of electrodes in the ROI classified in the category divided by the total number of electrodes in the ROI. The total numbers and percentages of electrodes in each region and electrophysiological category are listed in Table 1.

Table 1
Distribution of significant changes in power spectra related to memory load across all subjects in the 6 regions and 3 electrophysiological categories

ROI	Total # elec.	# T/A inc.	% T/A inc.	# T/A dec.	% T/A dec.	# G inc.	% G dec.
ML	255	53	21	21	8	44	17
OC	135	11	8	44	33	47	35
LF	230	31	13	50	22	27	12
RF	268	24	9	36	13	32	12
LT	265	25	9	27	10	38	14
RT	300	28	9	26	9	33	11

Note: The columns show the total number of electrodes in each ROI, and the number and percentage of electrodes showing theta/alpha increase, theta/alpha decrease, and gamma increase.

Figure 4*B* indicates that electrodes in the ML region were approximately twice as likely to exhibit an increase in theta/alpha power with memory load than electrodes in other regions. The Mantel–Haenszel test (see Methods) was used to evaluate that conclusion statistically, while controlling for the effect of different electrode arrangements in different subjects. Mantel–Haenszel tests were carried out on each of the 3 electrophysiological categories, testing for a difference between the ML ROI and all others combined. As hypothesized, there was a significant effect only for theta/alpha increase (Mantel–Haenzel $\chi^2(\text{df} = 1) = 10.33$, $P = 0.0013$). The common odds ratio for theta/alpha increase in the ML ROI versus the other regions was 2.04, confirming that electrodes in this region are twice as likely to exhibit a theta/alpha increase, regardless of subject effects. No effect was found for theta/alpha decrease ($\chi^2(\text{df} = 1) = 0.14$, not significant [NS]) or for gamma increase ($\chi^2(\text{df} = 1) = 1.03$, NS).

The proportions of electrodes in each electrophysiological category for each of the 6 ROIs are presented in Figure 4*C*, so that any other salient tendencies of anatomical distribution may be detected. Cochran–Mantel–Haenzel tests were conducted including the 6 ROIs as a categorical factor. Significant effects of ROI were detected for all 3 electrophysiological categories, and were particularly strong for the theta/alpha decrease and gamma increase:

1. theta/alpha increase: $M^2(\text{df} = 5) = 13.42$, $P = 0.0198$
2. theta/alpha decrease: $M^2(\text{df} = 5) = 59.87$, $P < 0.0001$
3. theta/alpha decrease: $M^2(\text{df} = 5) = 59.39$, $P < 0.0001$

Inspection of the graph in Figure 4*C*, as well as the spatial maps in Figure 5 (see below), indicates that the effect of ROI for both theta/alpha decrease and gamma increase is primarily attributable to the prevalence of both of these effects in the occipital region. Furthermore, these 2 effects appear to occur at the exact same electrode sites. To assess that impression statistically, we conducted a Mantel–Haenzel test for an association between gamma increase and theta/alpha decrease as categorical factors, which was significant ($\chi^2(\text{df} = 1) = 10.51$, $P = 0.0012$, common odds ratio = 1.86), indicating that an electrode with a theta/alpha decrease was almost twice as likely to exhibit a gamma increase as well (and vice versa). When occipital electrodes were removed from the data set, however, there was no longer any significant association, suggesting that the link between theta/alpha decrease and gamma increase may be specific to that region. In contrast, there was no significant association between theta/alpha increase and gamma increase ($\chi^2(\text{df} = 1) = 1.54$, NS). Even though a relatively large number of electrodes in the frontal midline region tended to exhibit increases in gamma power, these electrodes did not tend to be the exact same ones at which theta/alpha power increased, a fact best appreciated by visual inspection of Figure 5.

Maps of electrode locations for power spectral changes in all 3 categories are displayed in Figure 5, overlaid on the fMRI map of memory load–induced changes in BOLD signal from our previous study of the Sternberg task (Meltzer et al. 2007). Figure 5*A* displays electrodes showing an increase in theta/alpha power with memory load. As predicted, a high concentration of these occurs in the frontal midline region. However, increases are also detected in many other regions, including lateral posterior parietal regions. Notably, increases in theta/alpha power are largely absent from lateral frontal regions.

Figure 5*B* displays electrodes showing a decrease in theta/alpha power. These locations of the decreases do not display much overlap with the increases, confirming the anatomical dissociation between the effects obtained in the categorical analysis. Decreases in theta/alpha power are highly concentrated in the occipital lobe, but also occur in lateral frontal and anterior parietal regions. The most salient correspondence between positive BOLD activation and EEG reactivity appears to occur in the left precentral gyrus, although electrodes exhibiting theta/alpha decreases also occur in surrounding areas not characterized by a significant BOLD response on the group level.

Locations of gamma power increases are plotted in Figure 5*C*. As indicated in the categorical analysis, gamma increases occurred most commonly in the occipital lobe, colocalized with theta/alpha decreases. Gamma increases also occur in other regions, including both the left precentral gyrus (colocalized with theta/alpha decreases) and the frontal midline cortex. However, the electrodes with gamma power increases in frontal midline cortex did not tend to overlap those characterized by theta/alpha increase, being located somewhat more posteriorly within the midline region.

Discussion

This study explored the relationship between memory load and neuronal oscillatory power in different frequency bands, employing human intracranial recordings in a task that has been previously studied with fMRI, EEG, and MEG. Invasive recordings in humans, despite their numerous drawbacks, have the potential to reveal activity that is not readily detectable in surface recordings, particularly activity that is coherent over a smaller spatial scale. Scalp recordings tend to be dominated by large-scale coherent oscillations, which mainly occur at low frequencies, both spatial and temporal (Nunez et al. 2001). Therefore, intracranial EEG may be more sensitive to activity in higher frequency bands than both scalp EEG and MEG. Given that fMRI signals have been shown to increase with memory load in several brain regions (Rypma et al. 1999; Jha and McCarthy 2000; Kirschen et al. 2005; Narayanan et al. 2005; Zarahn et al. 2005), and that gamma oscillations have been shown to be positively associated with BOLD signal changes measured in fMRI (Brookes et al. 2005; Mukamel et al. 2005; Niessing et al. 2005), it may be expected that increases in gamma oscillations with memory load could be detected in intracranial recordings. This was demonstrated in the study of Howard et al. (2003), and replicated in the current study. Increases in gamma power have been reported in numerous other EEG studies of cognitive tasks (for review, see Kaiser and Lutzenberger 2005), and it is relatively uncontroversial that gamma oscillations index neuronal activity of cognitive relevance.

The role of lower frequency oscillations in cognition is much less clear. Traditionally, alpha oscillations have been considered to index an "idling" state of cortex, as they tend to increase in amplitude during conditions of lower cognitive demand (Pfurtscheller et al. 1996; Gevins et al. 1997). However, numerous exceptions have been reported, where cognitive tasks induce increases in alpha power (Klimesch et al. 1999; Bastiaansen et al. 2002). Two noninvasive studies of the Sternberg task have reported increases in lower frequency power with memory load: alpha in an EEG study (Jensen et al.

2002), and theta in an MEG study (Jensen and Tesche 2002). As discussed in the introduction, both theta and alpha oscillations have been shown to correlate negatively with BOLD in simultaneous EEG/fMRI studies. Therefore, it is likely that the increased theta and alpha power occurring in the Sternberg task originates in regions other than those that generate positive BOLD signals. Increased theta oscillations have been reported in numerous cognitive tasks, and are commonly localized to the medial prefrontal cortex (Asada et al. 1999; Ishii et al. 1999). Interestingly, this region frequently exhibits decreases in BOLD in a wide variety of cognitive paradigms (Gusnard and Raichle 2001). On the basis of these findings, we hypothesized that the relationship between low-frequency oscillations and cognitive demand may vary regionally in the brain, just as the BOLD signal does, tending to increase in some regions and decrease in others.

Human intracranial recordings are ideally suited for the investigation of anatomical dissociations in the role of brain oscillations. One disadvantage of scalp recordings is that activity from multiple brain regions is mixed at scalp sensors. Although intracranial recordings may also reflect activity mixed from multiple sources, they may offer a somewhat more localized view of activity, given that the electrical fields are not "smeared" by passing through the skull. Interestingly, a recent study that also examined theta oscillations in the Sternberg task reported a general lack of coherence between distant electrodes exhibiting task-modulated theta oscillations, suggesting that these recordings are sensitive to activity largely of local origin (Raghavachari et al. 2006). Therefore, an intracranial study may be expected to yield information on the anatomical distribution of cognitive effects on neuronal oscillations in different frequency bands, complementary to that obtained from noninvasive recordings. In this study, we have focused on the changes in spectral power occurring at each electrode, in order to answer specific questions about the anatomical distribution of such changes and their potential relationship to other modalities of neuroimaging. However, we note that several other techniques are available for the analysis of scalp and intracranial EEG data, such as event-related potentials, coherence between multiple electrodes (Nunez et al. 1997), and nonlinear dynamical methods (Stam 2005). Such techniques have the potential to yield additional information useful for the interpretation of large-scale field potentials recorded during cognitive tasks.

Consistent with an earlier report (Howard et al. 2003), we found that power in the gamma band tended to increase with working-memory load. However, the gamma band effects were not the only salient effects in the current study, as we also detected a similar proportion of electrodes at which power in lower frequency bands was modulated by memory load. Both increases and decreases were observed in a broad range that included both the theta and alpha bands, as traditionally defined. This pattern of results suggests that there is no single relationship between low-frequency oscillations and cognitive demand, in contrast to the gamma band, in which load-related changes were predominantly positive. Rather, increases and decreases in low-frequency power may index qualitatively different phenomena, both of which play a role in working memory. Just as cognitive demands may induce both increases and decreases in BOLD in different areas, changes in low-frequency power of opposite sign may reflect different neuronal processes that are dissociable on other criteria.

The most easily detectable form of a dissociation between power changes of opposite sign would be complementary anatomical distributions. Although we did not observe a complete lack of overlap between increases and decreases in theta/alpha power, the localizations of these 2 effects were statistically separable. As hypothesized, increases in theta/alpha power occurred in the frontal/parietal midline regions significantly more often than in other regions. These regions frequently exhibit decreases in BOLD signal with increasing cognitive demands (Gusnard and Raichle 2001; McKiernan et al. 2003). Although the fMRI map shown as the underlay in Figure 5 does not display fMRI deactivation in medial prefrontal cortex, that is because it is the map of effects that were significant across the entire cohort of subjects. In the previous EEG/fMRI study of individual differences (Meltzer et al. 2007), we specifically found that the minority of subjects exhibiting load-dependent increases in theta power were the same ones that exhibited medial prefrontal deactivation. The present finding of theta/alpha increases in commonly deactivated regions provides additional evidence that negative BOLD and low-frequency oscillatory synchronization both reflect a form of neural activity characterized by a lower rate of metabolic demand, as indexed by fMRI and PET. Similarly, it is likely that the observed increases in medial prefrontal theta in this study arise from a subset of the subjects. Nonetheless, it is likely that task-induced low-frequency oscillations in medial prefrontal cortex play an important computational role in cognition, as several recent studies have demonstrated that theta oscillations coordinate neuronal activity between medial prefrontal cortex and hippocampus in rodents (Hyman et al. 2005; Jones and Wilson 2005; Siapas et al. 2005). Notably, theta activity in rodents is conventionally defined as 4–12 Hz, which includes both the theta and alpha bands in human EEG terminology. Rodent studies have also demonstrated an inverse correlation between theta power and metabolism, despite increases in theta power under conditions of greater cognitive demand (Sanchez-Arroyos et al. 1993; Uecker et al. 1997).

The tendency of load-induced theta/alpha power increases to occur in midline regions may explain why they were not observed in several previous intracranial studies of the Sternberg task (Raghavachari et al. 2001; Howard et al. 2003; Rizzuto et al. 2003; Raghavachari et al. 2006). In all of those studies, very few recordings from midline electrodes were obtained, whereas all of our patients had some electrodes implanted subdurally within the longitudinal fissure separating the 2 brain hemispheres. Most likely, this reflects differences in clinical practice between our neurosurgical team in New Haven and the team in Boston that implanted the electrodes used in the previous studies. Although in both cases electrode placement was defined strictly by clinical criteria, practices do vary at different hospitals. However, other important differences exist between our study and previous studies. We presented the digits to be encoded simultaneously in one array, whereas the previous studies presented them sequentially. In our case, this was done so that the intracranial study would be directly comparable with our EEG–fMRI study, which used simultaneous presentation. Additionally, our study used a much longer delay period of 6 s.

Decreases in theta/alpha power, although as common as increases, tended to occur in different regions than the increases, and were most prevalent in occipital cortex. Gamma increases were also most frequent in the same region, and often occurred

at the exact same electrode sites. This finding suggests that decreases in lower frequencies and increases in higher frequencies may both reflect the same underlying neural activity, which occurs preferentially in the occipital lobe. A recent theoretical investigation suggested that neuronal "activation" is characterized by an overall acceleration of temporal dynamics leading to a shift away from lower frequencies toward higher frequencies (Kilner et al. 2005), thus predicting that theta/alpha decreases should colocalize with gamma increases. Our data support this hypothesis in the occipital lobe, but do not provide strong evidence for or against it in other regions. Accordingly, an MEG study has also reported colocalization of alpha band decreases with gamma band increases and positive BOLD in occipital cortex (Brookes et al. 2005). Additionally, a recent MEG study employing a working-memory task with face stimuli (Jokisch and Jensen 2007) reported increases in occipital lobe gamma power during the retention interval, whereas increases in alpha power were localized to more dorsal parietal–occipital midline areas, consistent with our own observations that increases in these 2 frequency ranges tend not to overlap. At this point, it is uncertain why gamma modulations tend to be detected in the occipital lobe more than in other regions. One possibility is that gamma plays a special role in primary visual processing that is not generalized to other cognitive and anatomical domains, although gamma activity in primary auditory cortex is also well documented (Sekihara et al. 2000; Mukamel et al. 2005). Jokisch and Jensen (2007) suggest that the failure to observe gamma modulations in more anterior areas such as the fusiform gyrus may be due to the distance of those areas from the MEG sensors. However, in our intracranial study, increases in gamma power were predominantly detected in occipital cortex (although not exclusively) despite extensive coverage of other brain regions involved in working memory, suggesting that gamma oscillations are in fact more prevalent in the occipital lobe, rather than being preferentially detected there due to anatomical biases present in noninvasive sensor arrangements.

Additionally, we shall discuss the relationship between the current findings on the Sternberg task and existing findings on one other cognitive paradigm, in which neuronal oscillations have been extensively investigated: subsequent memory effects. In this paradigm, words or pictures are presented for memory encoding, and the subject is tested later on their ability to recall them. Items are retrospectively classified as remembered or forgotten (further categorizations may also be made), and activity that predicts successful or unsuccessful memory formation is identified. Numerous fMRI studies have identified increases in BOLD activity predictive of subsequent memory (Brewer et al. 1998; Wagner et al. 1998; Reber et al. 2002; Davachi et al. 2003). Intracranial EEG (Sederberg et al. 2003, 2006) and MEG studies (Osipova et al. 2006) have both detected significant increases in gamma activity for subsequently remembered items, localized to occipital cortex (and other regions in the case of the intracranial studies). In the theta band, numerous studies have reported positive subsequent memory effects (intracranial EEG: Sederberg et al. 2003; MEG: Osipova et al. 2006; EEG: Klimesch et al. 1996), although negative effects (Sederberg et al. 2006) have also been reported in the same frequency range. Localization of positive subsequent memory effects in the theta band has not been extensively characterized, but it is possible these effects may also correspond to negative BOLD effects, as 2 studies have demonstrated negative subsequent memory effects in fMRI (Otten and Rugg 2001; Daselaar et al. 2004), localized to posterior midline, prefrontal, and inferior parietal regions. This possibility awaits further study.

One surprising outcome of this study is that there did not seem to be any tight spatial correspondence between the patterns of intracranial EEG reactivity and BOLD responses obtained from the earlier EEG–fMRI study (Meltzer et al. 2007), as displayed in Figure 5. There are several possible reasons for this. The simplest explanation is that fMRI and EEG responses are independent phenomena, reflecting separate aspects of neuronal activity that do not necessarily occur at the same region. However, even if electrophysiological and hemodynamic responses are linked in certain cases, other factors may prevent a tight colocalization in comparisons of fMRI and intracranial EEG. One simple reason is that the electrodes are not actually located within the cortex where BOLD signal changes are generated; rather, they are in the subdural space several millimeters away from the BOLD maxima. Thus, any signal detected by these electrodes is unlikely to be generated at the site of the electrode, but instead is volume-conducted from adjacent tissue of unknown spatial extent. Thus, in Figure 5*B*,*C*, we see a large number of occipital electrodes exhibiting theta/alpha decreases and gamma increases. These are located close to a large cluster of BOLD activation, but not exactly within that cluster. Similarly, the frontal midline electrodes exhibiting increases in theta/alpha power are mostly located at the frontal pole, not within the midline cortex lining the longitudinal fissure where negative correlations between EEG theta and BOLD were observed in the companion fMRI study (Meltzer et al. 2007). Therefore, it is impossible to say with certainty whether the BOLD activation and the EEG dynamics are independent effects, or if they are representative of the same neural activity, reflected via volume conduction in electrodes somewhat removed from the BOLD activation. Notably, the same uncertainty would apply even if the electrodes and the BOLD were perfectly colocalized, as the electrodes could be detecting activity originating in areas outside the BOLD activation.

Another factor differentiating the EEG results from the fMRI map is that the fMRI map is a group average of effects that are significant on the population level, derived from a cohort analysis. The EEG electrodes that are highlighted were significant in an individual subject. Although the large-scale lobar-level categorical tests took this into account, the maps do not, and hence there is no guarantee that most subjects would exhibit a significant change in EEG dynamics on an electrode located in the same location. Thus, it is possible that the large spread in the locations of EEG effects seen in Figure 5 may be matched by a large spread in individual fMRI reactivity that is not reflected in the results of the cohort-level random effects analysis. In the present results, the closest match between BOLD activation and EEG dynamics appears to be the theta/alpha decrease in the left precentral gyrus. However, the number of subjects with electrodes overlying that region is not large enough to conclude an invariable association between those 2 effects. The occurrence of EEG responses in many other locations not accompanied by BOLD responses on the cohort level suggests that EEG and fMRI reactivity may dissociable to some extent, with a significant change occurring in either modality without the other.

In summary, we have found that gamma oscillations tend to increase with greater working-memory load, preferentially in occipital cortex, whereas lower frequency oscillations in the theta/alpha range exhibit 2 different patterns: increases with memory load, localized preferentially to midline cortical regions, and decreases with memory load, which tend to colocalize with gamma increases in occipital cortex, but also colocalize with positive BOLD responses in the precentral gyrus. Additionally, we found that oscillatory reactivity may occur in widespread regions of the cortex not necessarily colocalized with fMRI activation observed consistently in normals performing the same task. These findings underscore the danger inherent in ascribing a single functional role to oscillations within a given frequency band, as the behavior of a certain frequency band can be very different across brain regions, even within the same task comparison. As recent years have seen the introduction of several new methods for noninvasive mapping of oscillatory activity in the brain with reasonable accuracy (Hillebrand and Barnes 2005; Liljestrom et al. 2005), one can expect that neuroanatomical distinctions such as these will play a key role in elucidating the role of oscillatory neuronal activity in human cognition.

Funding

National Institutes of Health grants (RO1 NS051622 to RTC and RO1 EB006494 to XP); and American Epilepsy Society predoctoral training fellowship to J.A.M.

Notes

We thank the staff of the Yale Epilepsy Monitoring Unit for their help and support, and gratefully acknowledge the assistance of Brad Duckrow, Hal Blumenfeld, Dave Ocame, and Sarah Iverson in accommodating our study. Most of all we thank the participating patients and their families. *Conflict of Interest*: None declared.

Address correspondence to Jed A. Meltzer, PhD, National Institute on Deafness and Other Communication Disorders, National Institutes of Health, Building 10, room 5C410, 10 Center Drive, Bethesda, MD 20852, USA. Email: jed.meltzer@aya.yale.edu.

References

Agresti A. 2002. Categorical data analysis. Hoboken (NJ): Wiley.

Asada H, Fukuda Y, Tsunoda S, Yamaguchi M, Tonoike M. 1999. Frontal midline theta rhythms reflect alternative activation of prefrontal cortex and anterior cingulate cortex in humans. Neurosci Lett. 274:29–32.

Axmacher N, Mormann F, Fernandez G, Cohen MX, Elger CE, Fell J. 2007. Sustained neural activity patterns during working memory in the human medial temporal lobe. J Neurosci. 27:7807–7816.

Bastiaansen MC, Posthuma D, Groot PF, de Geus EJ. 2002. Event-related alpha and theta responses in a visuo-spatial working memory task. Clin Neurophysiol. 113:1882–1893.

Brewer JB, Zhao Z, Desmond JE, Glover GH, Gabrieli JD. 1998. Making memories: brain activity that predicts how well visual experience will be remembered. Science. 281:1185–1187.

Brookes MJ, Gibson AM, Hall SD, Furlong PL, Barnes GR, Hillebrand A, Singh KD, Holliday IE, Francis ST, Morris PG. 2005. GLM-beamformer method demonstrates stationary field, alpha ERD and gamma ERS co-localisation with fMRI BOLD response in visual cortex. Neuroimage. 26:302–308.

Ciulla C, Takeda T, Endo H. 1999. MEG characterization of spontaneous alpha rhythm in the human brain. Brain Topogr. 11:211–222.

Daselaar SM, Prince SE, Cabeza R. 2004. When less means more: deactivations during encoding that predict subsequent memory. Neuroimage. 23:921–927.

Davachi L, Mitchell JP, Wagner AD. 2003. Multiple routes to memory: distinct medial temporal lobe processes build item and source memories. Proc Natl Acad Sci USA. 100:2157–2162.

Delorme A, Makeig S. 2004. EEGLAB: an open source toolbox for analysis of single-trial EEG dynamics including independent component analysis. J Neurosci Methods. 134:9–21.

Foucher JR, Otzenberger H, Gounot D. 2003. The BOLD response and the gamma oscillations respond differently than evoked potentials: an interleaved EEG-fMRI study. BMC Neurosci. 4:22.

Fox MD, Snyder AZ, Vincent JL, Corbetta M, Van Essen DC, Raichle ME. 2005. The human brain is intrinsically organized into dynamic, anticorrelated functional networks. Proc Natl Acad Sci USA. 102:9673–9678.

Gevins A, Smith ME, McEvoy L, Yu D. 1997. High-resolution EEG mapping of cortical activation related to working memory: effects of task difficulty, type of processing, and practice. Cereb Cortex. 7:374–385.

Goldman RI, Stern JM, Engel J, Jr, Cohen MS. 2002. Simultaneous EEG and fMRI of the alpha rhythm. Neuroreport. 13:2487–2492.

Gusnard DA, Raichle ME. 2001. Searching for a baseline: functional imaging and the resting human brain. Nat Rev Neurosci. 2:685–694.

Hillebrand A, Barnes GR. 2005. Beamformer analysis of MEG data. Int Rev Neurobiol. 68:149–171.

Howard MW, Rizzuto DS, Caplan JB, Madsen JR, Lisman J, Aschenbrenner-Scheibe R, Schulze-Bonhage A, Kahana MJ. 2003. Gamma oscillations correlate with working memory load in humans. Cereb Cortex. 13:1369–1374.

Hyman JM, Zilli EA, Paley AM, Hasselmo ME. 2005. Medial prefrontal cortex cells show dynamic modulation with the hippocampal theta rhythm dependent on behavior. Hippocampus. 15:739–749.

Ishii R, Shinosaki K, Ukai S, Inouye T, Ishihara T, Yoshimine T, Hirabuki N, Asada H, Kihara T, Robinson SE, Takeda M. 1999. Medial prefrontal cortex generates frontal midline theta rhythm. Neuroreport. 10:675–679.

Jensen O, Gelfand J, Kounios J, Lisman JE. 2002. Oscillations in the alpha band (9-12 Hz) increase with memory load during retention in a short-term memory task. Cereb Cortex. 12:877–882.

Jensen O, Tesche CD. 2002. Frontal theta activity in humans increases with memory load in a working memory task. Eur J Neurosci. 15:1395–1399.

Jha AP, McCarthy G. 2000. The influence of memory load upon delay-interval activity in a working-memory task: an event-related functional MRI study. J Cogn Neurosci. 12(Suppl 2):90–105.

Jokisch D, Jensen O. 2007. Modulation of gamma and alpha activity during a working memory task engaging the dorsal or ventral stream. J Neurosci. 27:3244–3251.

Jones MW, Wilson MA. 2005. Theta rhythms coordinate hippocampal-prefrontal interactions in a spatial memory task. PLoS Biol. 3:e402.

Kaiser J, Lutzenberger W. 2005. Human gamma-band activity: a window to cognitive processing. Neuroreport. 16:207–211.

Kilner JM, Mattout J, Henson R, Friston KJ. 2005. Hemodynamic correlates of EEG: a heuristic. Neuroimage. 28:280–286.

Kirschen MP, Chen SH, Schraedley-Desmond P, Desmond JE. 2005. Load- and practice-dependent increases in cerebro-cerebellar activation in verbal working memory: an fMRI study. Neuroimage. 24:462–472.

Klimesch W, Doppelmayr M, Russegger H, Pachinger T. 1996. Theta band power in the human scalp EEG and the encoding of new information. Neuroreport. 7:1235–1240.

Klimesch W, Doppelmayr M, Schwaiger J, Auinger P, Winkler T. 1999. 'Paradoxical' alpha synchronization in a memory task. Brain Res Cogn Brain Res. 7:493–501.

Laufs H, Kleinschmidt A, Beyerle A, Eger E, Salek-Haddadi A, Preibisch C, Krakow K. 2003. EEG-correlated fMRI of human alpha activity. Neuroimage. 19:1463–1476.

Liljestrom M, Kujala J, Jensen O, Salmelin R. 2005. Neuromagnetic localization of rhythmic activity in the human brain: a comparison of three methods. Neuroimage. 25:734–745.

Luu P, Tucker DM, Makeig S. 2004. Frontal midline theta and the error-related negativity: neurophysiological mechanisms of action regulation. Clin Neurophysiol. 115:1821–1835.
Mainy N, Kahane P, Minotti L, Hoffmann D, Bertrand O, Lachaux JP. 2007. Neural correlates of consolidation in working memory. Hum Brain Mapp. 28:183–193.
Makeig S. 1993. Auditory event-related dynamics of the EEG spectrum and effects of exposure to tones. Electroencephalogr Clin Neurophysiol. 86:283–293.
McKiernan KA, Kaufman JN, Kucera-Thompson J, Binder JR. 2003. A parametric manipulation of factors affecting task-induced deactivation in functional neuroimaging. J Cogn Neurosci. 15:394–408.
Meltzer JA, Negishi M, Mayes LC, Constable RT. 2007. Individual differences in EEG theta and alpha dynamics during working memory correlate with fMRI responses across subjects. Clin Neurophysiol. 118:2419–2436.
Mizuhara H, Wang LQ, Kobayashi K, Yamaguchi Y. 2004. A long-range cortical network emerging with theta oscillation in a mental task. Neuroreport. 15:1233–1238.
Moosmann M, Ritter P, Krastel I, Brink A, Thees S, Blankenburg F, Taskin B, Obrig H, Villringer A. 2003. Correlates of alpha rhythm in functional magnetic resonance imaging and near infrared spectroscopy. Neuroimage. 20:145–158.
Mukamel R, Gelbard H, Arieli A, Hasson U, Fried I, Malach R. 2005. Coupling between neuronal firing, field potentials, and FMRI in human auditory cortex. Science. 309:951–954.
Narayanan NS, Prabhakaran V, Bunge SA, Christoff K, Fine EM, Gabrieli JD. 2005. The role of the prefrontal cortex in the maintenance of verbal working memory: an event-related FMRI analysis. Neuropsychology. 19:223–232.
Niessing J, Ebisch B, Schmidt KE, Niessing M, Singer W, Galuske RA. 2005. Hemodynamic signals correlate tightly with synchronized gamma oscillations. Science. 309:948–951.
Nunez PL, Srinivasan R, Westdorp AF, Wijesinghe RS, Tucker DM, Silberstein RB, Cadusch PJ. 1997. EEG coherency. I: Statistics, reference electrode, volume conduction, Laplacians, cortical imaging, and interpretation at multiple scales. Electroencephalogr Clin Neurophysiol. 103:499–515.
Nunez PL, Wingeier BM, Silberstein RB. 2001. Spatial-temporal structures of human alpha rhythms: theory, microcurrent sources, multiscale measurements, and global binding of local networks. Hum Brain Mapp. 13:125–164.
Onton J, Delorme A, Makeig S. 2005. Frontal midline EEG dynamics during working memory. Neuroimage. 27:341–356.
Osipova D, Takashima A, Oostenveld R, Fernandez G, Maris E, Jensen O. 2006. Theta and gamma oscillations predict encoding and retrieval of declarative memory. J Neurosci. 26:7523–7531.
Otten LJ, Rugg MD. 2001. When more means less: neural activity related to unsuccessful memory encoding. Curr Biol. 11:1528–1530.
Papademetris X, Jackowski AP, Schultz RT, Staib LH, Duncan JS. 2004. Integrated intensity and point-feature non-rigid registration. In: Barillot C, Haynor D, Hellier P, editors. Medical image computing and computer-assisted intervention. Saint_malo, France: Springer. pp. 763–770.
Pfurtscheller G, Stancak A, Jr, Neuper C. 1996. Event-related synchronization (ERS) in the alpha band—an electrophysiological correlate of cortical idling: a review. Int J Psychophysiol. 24:39–46.
Raghavachari S, Kahana MJ, Rizzuto DS, Caplan JB, Kirschen MP, Bourgeois B, Madsen JR, Lisman JE. 2001. Gating of human theta oscillations by a working memory task. J Neurosci. 21:3175–3183.
Raghavachari S, Lisman JE, Tully M, Madsen JR, Bromfield EB, Kahana MJ. 2006. Theta oscillations in human cortex during a working-memory task: evidence for local generators. J Neurophysiol. 95:1630–1638.
Reber PJ, Siwiec RM, Gitelman DR, Parrish TB, Mesulam MM, Paller KA, Gitleman DR. 2002. Neural correlates of successful encoding identified using functional magnetic resonance imaging. J Neurosci. 22:9541–9548.
Rizzuto DS, Madsen JR, Bromfield EB, Schulze-Bonhage A, Seelig D, Aschenbrenner-Scheibe R, Kahana MJ. 2003. Reset of human neocortical oscillations during a working memory task. Proc Natl Acad Sci USA. 100:7931–7936.
Rypma B, Prabhakaran V, Desmond JE, Glover GH, Gabrieli JD. 1999. Load-dependent roles of frontal brain regions in the maintenance of working memory. Neuroimage. 9:216–226.
Sanchez-Arroyos R, Gaztelu JM, Zaplana J, Dajas F, Garcia-Austt E. 1993. Hippocampal and entorhinal glucose metabolism in relation to cholinergic theta rhythm. Brain Res Bull. 32:171–178.
Sederberg PB, Kahana MJ, Howard MW, Donner EJ, Madsen JR. 2003. Theta and gamma oscillations during encoding predict subsequent recall. J Neurosci. 23:10809–10814.
Sederberg PB, Gauthier LV, Terushkin V, Miller JF, Barnathan JA, Kahana MJ. 2006. Oscillatory correlates of the primacy effect in episodic memory. Neuroimage. 32:1422–1431.
Sekihara K, Nagarajan SS, Poeppel D, Miyauchi S, Fujimaki N, Koizumi H, Miyashita Y. 2000. Estimating neural sources from each time-frequency component of magnetoencephalographic data. IEEE Trans Biomed Eng. 47:642–653.
Shulman GL, Fiez JA, Corbetta M, Buckner RL, Miezin FM, Raichle ME, Petersen SE. 1997. Common blood flow changes across visual tasks: II. Decreases in cerebral cortex. J Cogn Neurosci. 9:648–663.
Siapas AG, Lubenov EV, Wilson MA. 2005. Prefrontal phase locking to hippocampal theta oscillations. Neuron. 46:141–151.
Singh KD, Barnes GR, Hillebrand A, Forde EM, Williams AL. 2002. Task-related changes in cortical synchronization are spatially coincident with the hemodynamic response. Neuroimage. 16:103–114.
Stam CJ. 2005. Nonlinear dynamical analysis of EEG and MEG: review of an emerging field. Clin Neurophysiol. 116:2266–2301.
Tsujimoto T, Shimazu H, Isomura Y. 2006. Direct recording of theta oscillations in primate prefrontal and anterior cingulate cortices. J Neurophysiol. 95:2987–3000.
Tuladhar AM, Huurne NT, Schoffelen JM, Maris E, Oostenveld R, Jensen O. 2007. Parieto-occipital sources account for the increase in alpha activity with working memory load. Hum Brain Mapp. 31:31.
Uchida S, Maehara T, Hirai N, Kawai K, Shimizu H. 2003. Theta oscillation in the anterior cingulate and beta-1 oscillation in the medial temporal cortices: a human case report. J Clin Neurosci. 10:371–374.
Uecker A, Barnes CA, McNaughton BL, Reiman EM. 1997. Hippocampal glycogen metabolism, EEG, and behavior. Behav Neurosci. 111:283–291.
Vanni S, Revonsuo A, Hari R. 1997. Modulation of the parieto-occipital alpha rhythm during object detection. J Neurosci. 17:7141–7147.
Wagner AD, Schacter DL, Rotte M, Koutstaal W, Maril A, Dale AM, Rosen BR, Buckner RL. 1998. Building memories: remembering and forgetting of verbal experiences as predicted by brain activity. Science. 281:1188–1191.
Wang C, Ulbert I, Schomer DL, Marinkovic K, Halgren E. 2005. Responses of human anterior cingulate cortex microdomains to error detection, conflict monitoring, stimulus-response mapping, familiarity, and orienting. J Neurosci. 25:604–613.
Yamagishi N, Callan DE, Goda N, Anderson SJ, Yoshida Y, Kawato M. 2003. Attentional modulation of oscillatory activity in human visual cortex. Neuroimage. 20:98–113.
Zarahn E, Rakitin B, Abela D, Flynn J, Stern Y. 2005. Positive evidence against human hippocampal involvement in working memory maintenance of familiar stimuli. Cereb Cortex. 15:303–316.